nature genetics

Insights from retinitis pigmentosa into the roles of isocitrate dehydrogenases in the Krebs cycle

Dyonne T Hartong[1,4,5], Mayura Dange[2,5], Terri L McGee[1], Eliot L Berson[3], Thaddeus P Dryja[1] & Roberta F Colman[2]

Here we describe two families with retinitis pigmentosa, a hereditary neurodegeneration of rod and cone photoreceptors in the retina. Affected family members were homozygous for loss-of-function mutations in *IDH3B*, encoding the β-subunit of NAD-specific isocitrate dehydrogenase (NAD-IDH, or IDH3), which is believed to catalyze the oxidation of isocitrate to α-ketoglutarate in the citric acid cycle. Cells from affected individuals had a substantial reduction of NAD-IDH activity, with about a 300-fold increase in the K_m for NAD. NADP-specific isocitrate dehydrogenase (NADP-IDH, or IDH2), an enzyme that catalyzes the same reaction, was normal in affected individuals, and they had no health problems associated with the enzyme deficiency except for retinitis pigmentosa. These findings support the hypothesis that mitochondrial NADP-IDH, rather than NAD-IDH, serves as the main catalyst for this reaction in the citric acid cycle outside the retina, and that the retina has a particular requirement for NAD-IDH.

Mutations in at least 34 genes have been identified as causes of nonsyndromic retinitis pigmentosa, including dominant mutations in 15 genes, recessive mutations in 20 genes and X-linked mutations in 2 genes (data from RetNet; see Methods for URL). The identified mutations are estimated to account for about 60% of cases of retinitis pigmentosa[1]. In addition, 11 unidentified genes have been mapped to specific chromosomal regions. There likely are dozens of unmapped, unidentified genes with recessive mutations associated with retinitis pigmentosa, each accounting for at most a few percent of cases[1,2].

We searched for some of these unidentified genes using an approach that relies on the fact that recessive alleles are often deletions, frameshift mutations or nonsense mutations that result in a scarcity of the disease gene's transcript because the transcript is either not made or rapidly degraded through nonsense-mediated decay[3]. The principle underlying this method has been described[4–6], but to our knowledge, the method has not been used to identify a human gene associated with a hereditary disease. Using microarray techniques that simultaneously assay mRNA levels from tens of thousands of transcripts in affected individuals, we searched for genes with absent or very low expression that may result from two allelic disease-causing mutations. It would have been ideal to carry out this analysis with RNA derived from the retina before its degeneration, but this tissue was not available from affected individuals. However, a substantial minority of the genes already known to be mutated in retinitis pigmentosa, including *RPGR*, *RP2*, *IMPDH1*, *PRPF31*, *PRPF8* and *PRPF3* (refs. 7–12), are expressed throughout the body, so we reasoned that low-abundance messages from some as-yet-unidentified genes might be detected by analyzing lymphoblast mRNA.

We focused our study on 13 unrelated families with recessive retinitis pigmentosa. The families were previously screened, with negative results, for mutations in all or all but one of the following genes associated with recessive retinitis pigmentosa: *PDE6A* (accounting for 3–4% of recessive retinitis pigmentosa cases), *PDE6B* (4–5%), *RPE65* (2%), *TULP1* (1%), *USH2A* (8%) and *CNGA1* (1%)[1]. Six of the 13 families had two or more available affected siblings: one sibship had four affected members, and five sibships each had two affected members. We preferred such multiplex sibships for this study, because if any of them had recessive mutations leading to low-abundance messages, the low-abundance mRNA would be shared by all affected siblings and would thus be more likely to be recognized as distinct from fortuitously low-abundance messages from genes other than the disease gene. We created lymphoblast cell lines from peripheral blood lymphocytes from the 13 index individuals, their available affected siblings and some unaffected relatives. We also prepared lymphoblast lines from four control individuals: two were unrelated individuals with Usher syndrome who were homozygous for the *USH2A* mutation 2299delG (E767SfsX21), one was an individual with dominant retinitis pigmentosa and the 68C>A (P23H) mutation of the rhodopsin gene, and one was an individual without retinitis pigmentosa or a family history of retinitis pigmentosa.

[1]Ocular Molecular Genetics Institute, Harvard Medical School, Massachusetts Eye and Ear Infirmary, 243 Charles Street, Boston, Massachusetts 02114, USA. [2]Department of Chemistry and Biochemistry, University of Delaware, Academy Street, Newark, Delaware 19716, USA. [3]The Berman-Gund Laboratory for the Study of Retinal Degenerations, Harvard Medical School, Massachusetts Eye and Ear Infirmary, 243 Charles Street, Boston, Massachusetts 02114, USA. [4]Present address: Department of Ophthalmology, University Medical Center Groningen, Groningen, The Netherlands. [5]These authors contributed equally to this work. Correspondence should be addressed to T.P.D. (thaddeus.dryja@novartis.com).

Received 18 March; accepted 1 July; published online 21 September 2008; doi:10.1038/ng.223

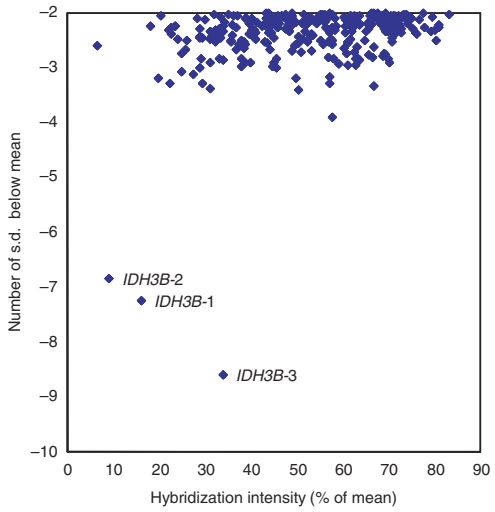

Figure 1 Scatter plot of probe-set hybridization intensities from individual 003-053. Data are organized according to percentage of respective mean signal across all subjects (*x* axis) and number of s.d. below this mean (*y* axis). The plot shows the 306 probe sets detecting hybridization signals two or more s.d. below the mean of all other subjects and controls. Of the 306 probe sets, 3 were clear outliers, with hybridization intensities more than 6 s.d. below the respective means; the 3 probe sets detected *IDH3B* (*IDH3B*-1, probe set 210014_x_at; *IDH3B*-2, 210418_s_at; *IDH3B*-3, 201509_at.) These were the only probe sets in the microarray designed to hybridize to mRNA from *IDH3B*.

Lymphoblast mRNA was labeled and hybridized to an Affymetrix U133 Plus 2.0 array, which has one or more sets of oligomer probes to individually assay over 47,000 human transcripts derived from approximately 39,500 genes or ESTs. Normalized signal intensities indicate the relative amount of mRNA bound to each probe. Applying stringent filtering criteria to the numerous genes in each lymphoblast line for which the microarray analysis indicated low mRNA levels, we identified 3 to 25 candidate genes or ESTs in each family, for an aggregate of 50 candidates in the multiplex families (**Supplementary Table 1** online). We individually eliminated 13 of the 50 corresponding genes as likely disease-associated genes because we found no mutations by direct sequencing or because our analysis of intragenic polymorphisms showed that the alleles did not segregate with disease among the relatives of the relevant index individual (**Supplementary Table 2** online). Analysis of the remaining candidate genes has not been completed.

We concurrently evaluated the microarray results from seven families in which only one affected individual provided a blood sample for a lymphoblast line. *IDH3B* (ref. 13) was the most notable gene from those families, as the three probe sets (210014_x_at, 210418_s_at and 201509_at) that hybridized to the *IDH3B* transcript in index individual 003-053 gave normalized hybridization signals of 62, 25 and 68, respectively; in contrast, the signals in the 24 other samples were 384 ± 44, 279 ± 37 and 200 ± 15.4 (mean ± s.d.), respectively (**Fig. 1**). Index individual 003-053 had an affected brother who had previously donated a blood sample for DNA analysis but had since died at age 71 years from carotid artery occlusion; lymphoblast cell lines had not been generated from this brother. Sequencing of *IDH3B* revealed that both the index individual and her deceased, affected brother were homozygous for a 1-bp deletion in codon 197 (589delA; p.I197fs; m.p.I163fs (m.p., mature protein); cDNA numbering is based on mRNA variant 1, which is the longest of the three known transcripts). The frameshift produced a premature stop codon in all three mRNA variants transcribed from *IDH3B* (**Fig. 2**). The parents of the affected individuals were first cousins. Four of the unaffected siblings were heterozygous, and one was wild type (**Fig. 3**).

We subsequently sequenced all 12 exons of *IDH3B* in 261 individuals with recessive retinitis pigmentosa and 285 individuals with simplex retinitis pigmentosa (most individuals with simplex retinitis pigmentosa have autosomal recessive disease). Individual 003-178 was homozygous for the m.p.L98P missense mutation (395T>C; p.L132P) in exon 5 (**Fig. 2**). This individual's parents were first cousins. The individual's three siblings, all unaffected, were heterozygous (**Fig. 3**). Neither the m.p.L98P mutation nor the m.p.I163fs mutation was found after screening leukocyte DNA from 95 control individuals without retinitis pigmentosa.

Individuals 003-053 and 003-178 were ophthalmologically examined at ages 47 and 38 years, respectively. Both had subnormal visual acuities, concentrically constricted visual fields, fundi typical of retinitis pigmentosa (pale optic discs, attenuated arterioles and intraretinal pigment deposits), impaired dark adaptation and reduced electroretinogram amplitudes indicating substantial loss of rod and cone photoreceptor function (see **Supplementary Note** online for clinical details.) They reported no other relevant health problems and, in particular, no problems typically associated with mitochondrial dysfunction (such as reduced muscle strength, cardiac dysrhythmias or reduced athletic stamina).

NAD-IDH is a heterotetramer with two α-subunits, one β-subunit and one γ-subunit[14]. In individual 003-053, who had the m.p.I163fs mutation, the β-subunit is presumably poorly expressed (as indicated by the low message levels detected by the microarray analysis). Any *IDH3B*-encoded protein produced would be truncated and unlikely to participate in a functional heterotetramer. To confirm this prediction and determine the effect of the substitution m.p.L98P, we evaluated NAD-IDH activity in lymphoblast cell lysates from the index individuals, some of their heterozygous siblings and unaffected individuals. The NAD-IDH activities in homozygous cell lysates under standard assay conditions were only 4.8% (m.p.I163fs) and 2.4% (m.p.L98P) of normal control activity, whereas activities in heterozygous cell lysates

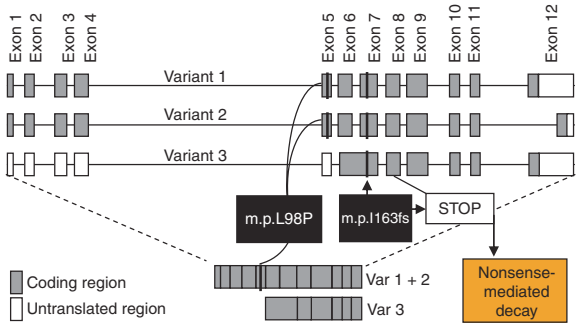

Figure 2 Structure of three known RNA splicing variants of *IDH3B*, and locations of the m.p.I163fs and m.p.L98P mutations. The m.p.L98P mutation leads to an amino acid substitution in IDH3B in variants 1 and 2. There is no predicted effect on variant 3, as the mutation is located in the 5′ untranslated region of this variant. Splice variant 3 is missing exons 1–5, which encode 132 amino acids of 385 in the full-length protein. It is not likely to encode a functional β-subunit that could compensate for the defective m.p.L98P protein in the two other variants. The m.p.I163fs mutation causes a frameshift with a premature stop codon in all three variants, presumably leading to mRNA degradation by nonsense-mediated decay.

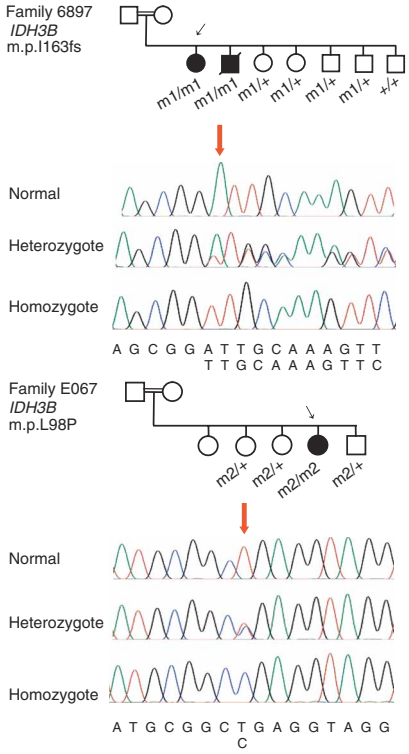

Figure 3 Pedigrees of two families with the *IDH3B* m.p.I163fs and m.p.L98P mutations. Black arrows point to the index individuals. Beneath each family member's symbol is that person's *IDH3B* genotype; family members for which no genotype is shown did not submit a blood sample for analysis. Red arrows indicate the location of the mutation in the DNA sequence traces. Nucleotides corresponding to the normal sequence (top line) and mutated sequences (lower line) are indicated below the sequence alignments. m.p.I163fs, m1; m.p.L98P, m2.

were 24% and 82%, respectively (**Fig. 4**). The K_m for NAD in homozygous lysates was 267- to 298-fold higher than normal, whereas the K_m in heterozygous lysates was 4- to 8-fold higher than normal (**Fig. 4**). The concentration of NAD in mammalian tissues has been estimated at 0.4–0.8 mM (ref. 15), which is sufficient for normal NAD-IDH (K_m for NAD ~40 μM) but too low to appreciably bind to the mutant NAD-IDH of homozygous lysates (K_m 11–12 mM).

Without ADP, the K_m for isocitrate was three- to four-fold higher than normal in homozygous cell lysates, whereas it was normal in heterozygous cell lysates (**Fig. 4**). ADP is an allosteric activator for IDH3, lowering its K_m for isocitrate[16]. In our assays on lysates from unaffected controls, ADP decreased the K_m for isocitrate to 11% of that in the absence of ADP, whereas in m.p.I163fs homozygous samples ADP only decreased the K_m for isocitrate to 35% of the value in its absence. This allosteric effect of ADP was almost completely lost in homozygous m.p.L98P mutant cells: ADP only lowered the K_m for isocitrate to 88% of the value obtained in its absence (**Fig. 4**). The importance of the region around m.p.L98P for activation of IDH by ADP is supported by previous studies of an engineered substitution of the neighboring residue m.p.Arg99 (p.Arg133). The mutant m.p.R99Q, like the m.p.L98P mutant, lacks an allosteric effect of ADP[17].

Figure 4 Activity of NAD-dependent isocitrate dehydrogenase. Shown are mean results of at least duplicate measurements of K_m for NAD and K_m for isocitrate (with or without ADP), V_{max} and NAD-IDH activity under standard conditions. Lymphoblast lysates were obtained from eight individuals: three unaffected (+/+), two heterozygous (m1/+) and one homozygous (m1/m1) for the *IDH3B* m.p.I163fs mutation, and one heterozygous (m2/+) and one homozygous (m2/m2) for the *IDH3B* m.p.L98P mutation. The individuals homozygous for either mutation had a 267- to 298-fold increase in the K_m for NAD (upper left) and a resulting loss of NAD-IDH activity (lower right). The normal effect of ADP in lowering the K_m for isocitrate is partially (for m1) or completely (for m2) lost in homozygous individuals (lower left). Error bars indicate s.d.

In the archetypical model of the citric acid cycle, also known as the Krebs cycle, NAD-IDH catalyzes the conversion of isocitrate to α-ketoglutarate, an essential reaction of the cycle that simultaneously changes a molecule of NAD^+ to NADH[18]. The NADH produced in this step and other steps of the citric acid cycle is used to generate ATP, a molecule universally used in cells as an energy source. It is therefore noteworthy that the individuals with homozygous *IDH3B* mutations had no evident health problems except for retinitis pigmentosa. Another mitochondrial enzyme, NADP-IDH, also converts isocitrate to α-ketoglutarate, but uses the cofactor $NADP^+$ instead of NAD^+. NADP-IDH activity and K_m were normal in the individuals with homozygous *IDH3B* mutations (**Supplementary Table 3** online). The NADPH produced by NADP-IDH can be converted into NADH through the action of nicotinamide-nucleotide transhydrogenase, which is present in the inner membrane of mitochondria[19,20]. The activity of NADP-IDH exceeds that of NAD-IDH in mammalian mitochondria[20], and the activity of the transhydrogenase is comparable to the rate of NADPH production by NADP-IDH. It is possible that, in the individuals with homozygous *IDH3B* mutations, NADP-IDH together with the transhydrogenase adequately substitute for the defective function of NAD-IDH in all tissues except the retina. In fact, our review of serial analysis of gene expression (SAGE) tags (EyeSAGE database; see Methods for URL), which crudely reflect mRNA expression levels, indicates that NADP-IDH tags are more frequent than NAD-IDH tags across all human tissues except the retina and retinal pigment epithelium (**Fig. 5**).

An alternative explanation for the viability of humans with greatly reduced NAD-IDH is that NADP-IDH may actually be the principal catalyst of the isocitrate to α-ketoglutarate reaction in the citric acid cycle in all tissues, whereas NAD-IDH serves as an accessory enzyme that augments or regulates the reaction, with the retina being particularly sensitive to the loss of this accessory activity. In this regard, it is notable that the K_m for isocitrate is about 1 μM for NADP-IDH, which is low relative to the 40–60 μM of isocitrate estimated to be present in mammalian mitochondria[21]. Thus,

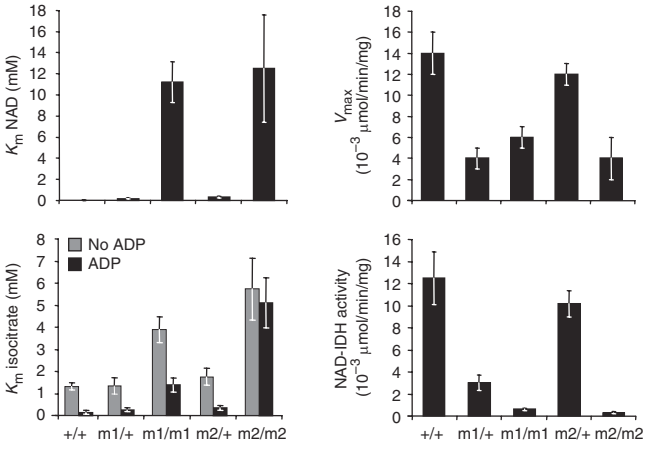

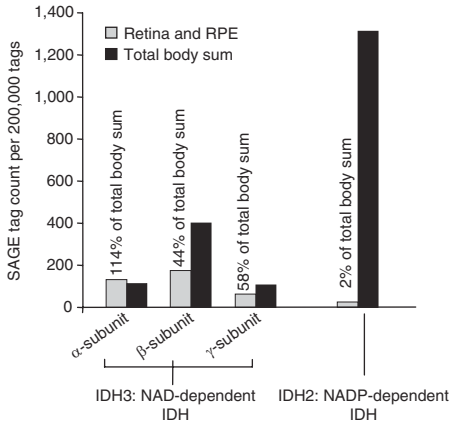

Figure 5 Frequency of SAGE tags from NAD-IDH (IDH3) and NADP-IDH (IDH2) in the retina and retinal pigment epithelium (RPE) compared to frequency from all other human tissues, using the EyeSAGE database. The low ratio of tags from NADP-IDH suggests that the retina and RPE have a relatively low abundance of NADP-IDH and are unusually dependent on NAD-IDH.

NADP-IDH would normally be saturated with isocitrate. Furthermore, the K_m for NADP is ~2 μM, whereas mammalian tissue levels of NADP are estimated at ~100 μM (ref. 15), so the coenzyme site would also be saturated. In contrast, the K_m of NAD-IDH for isocitrate is 1–2 mM (in the absence of ADP), which is high relative to the mitochondrial levels of isocitrate. It is only in the presence of ADP that the K_m for isocitrate is lowered to the 0.l-mM range, thereby allowing that enzyme to make a contribution to the oxidative decarboxylation of isocitrate. These considerations all support the interpretation that NADP-IDH is the major enzyme serving this step of the citric acid cycle, with the retina being a possible exception. The association of loss-of-function mutations with retinitis pigmentosa suggests that NAD-IDH is essential for normal retinal function. Further studies of mitochondrial metabolism in the retina and other tissues should help to confirm the association of NAD-IDH mutations with retinitis pigmentosa and the role of the IDH family of enzymes in mitochondrial metabolism.

METHODS

Subjects. Twenty-one individuals with recessive retinitis pigmentosa from 13 unrelated families and four control individuals were included in the study. This study adhered to the tenets of the Declaration of Helsinki and was approved by the Institutional Review Boards of the Massachusetts Eye and Ear Infirmary and Harvard Medical School and the Human Subjects Review Board of the University of Delaware. Informed consent was obtained from all study participants. See **Supplementary Note** for further details regarding subject recruitment and phenotyping criteria.

Lymphoblast cell lines. Cell lines were created from whole blood by immortalization with Epstein-Barr virus. Cells were grown to confluence, pelleted, suspended in TRIzol (Invitrogen) and stored at –80 °C until RNA was extracted.

RNA isolation, labeling and hybridization. Details in addition to those indicated in the text are provided in **Supplementary Methods** online.

Statistical analysis. Raw data reflecting hybridization intensities from individual probes of 25 different chips were provided as Microarray Suite 5.0 (Affymetrix) experiment data files (.chp, .txt, .rpt, .exp and .cel) and were normalized to a chip with median overall brightness using dChip[22]. The normalized data were extracted into a Microsoft Excel file, and hybridization intensities from all probes of the affected members of individual families were compared to all of the other samples. Significance in multiplex families was tested using a one-tailed Student's *t*-test assuming unequal variance, a Bonferroni correction and $P < 0.05$. In families with only one affected individual available, the transcript in that individual had to have a hybridization signal more than two s.d. below the mean hybridization intensity found in all other subjects.

DNA sequencing of candidate genes. Sequencing was done by amplifying individual exons along with flanking intron sequences using primers designed with Primer 3 (see below for URL). The amplified fragments were treated with ExoSAP-IT (US Biochemical) to eliminate unincorporated primers and dNTPs and then directly sequenced using BigDye version 3.1 and an ABI 3100 automated sequencer (Applied Biosystems). For some genes, only exons with one or more known SNPs were amplified and sequenced to determine whether the alleles segregated with disease in the relevant families. Primer sequences are listed in **Supplementary Table 4** online.

Protein extraction. Extraction was done by resuspending each lymphoblast cell pellet from a 200-ml culture (see **Supplementary Methods** for details of lymphoblast culture) in 1 ml of mammalian protein extraction reagent (Pierce). The volume of each cell pellet ranged from 300 to 400 μl and yielded between 9 and 15 mg of protein. The cells were incubated on ice during lysis for 1 h. The lysate was then centrifuged, and the supernatant was used for measuring enzyme activity and protein concentration. Protein concentration was determined from an absorbance at 280 nm after correcting for the ratio of the absorbances at 280 and 260 nm (ref. 23).

Activity of NAD-IDH and NADP-IDH. Activity was determined using the Perkin-Elmer fluorescence spectrophotometer MPF-3 by monitoring the time-dependent increase in the fluorescence of NADH or NADPH at 440 nm after excitation at 340 nm. Standard assay conditions for NAD-IDH were 33 mM Tris-acetate buffer (pH 7.2), 20 mM DL-isocitrate, 1 mM NAD and 1 mM $MnSO_4$ (final concentrations). Kinetic studies were conducted by varying the concentration of one substrate at a time. Measurements of the K_m for isocitrate in the absence and presence of 1 mM ADP were done at 10 mM NAD. Standard assay conditions for NADP-IDH were 30 mM triethanolamine hydrochloride buffer (pH 7.4), 4 mM DL-isocitrate, 0.1 mM NADP and 2 mM $MnSO_4$. The K_m values for isocitrate and for NADP were determined by varying the concentration of each substrate at otherwise standard conditions.

URLs. RetNet, http://www.sph.uth.tmc.edu/retnet/; EyeSAGE, http://neibank.nei.nih.gov/EyeSAGE/index.shtml; *IDH3B* splicing variants, http://genome.ucsc.edu/cgi-bin/hgTracks?position=chr20:2587041-2592843&hgsid=107503458&refGene=pack&hgFind.matches=NM_006899; Primer3, http://frodo.wi.mit.edu/cgi-bin/primer3/primer3_www.cgi.

Accession codes. Gene Expression Omnibus: mRNA expression data have been deposited with accession code GSE12086. Entrez Nucleotide for *IDH3B* (chromosome 20p13): NM_006899 (transcript variant 1), NM_174855 (transcript variant 2) and NM_174856 (transcript variant 3). Entrez Gene: 3491 (*IDH3A*, α-subunit), 3420 (*IDH3B*, β-subunit), 3421 (*IDH3G*, γ-subunit) and 3418 (*IDH2*). OMIM for *IDH3B*: 604526.

Note: Supplementary information is available on the Nature Genetics website.

ACKNOWLEDGMENTS

This work was supported by the Foundation Fighting Blindness and the US National Institutes of Health (NIH-EY00169, NIH-EY08683, NIH-HL67774 and P30-EY014104). The microarray analyses were carried out at the Microarray Core Facility at Dana-Farber Cancer Institute.

AUTHOR CONTRIBUTIONS

D.T.H., T.L.M. and T.P.D. designed and conducted the molecular genetic analyses. E.L.B. clinically evaluated, selected and recruited affected individuals and their family members and helped design the study. M.D. and R.F.C. designed and conducted the enzyme assays. All authors discussed and interpreted the results and wrote the manuscript.

COMPETING INTERESTS STATEMENT

The authors declare competing financial interests: details accompany the full-text HTML version of the paper at http://www.nature.com/naturegenetics/.

Published online at http://www.nature.com/naturegenetics/

1. Hartong, D.T., Berson, E.L. & Dryja, T.P. Retinitis pigmentosa. *Lancet* **368**, 1795–1809 (2006).
2. Daiger, S.P. Identifying retinal disease genes: how far have we come, how far do we have to go? *Novartis Found. Symp.* **255**, 17–27 (2004).
3. Losson, R. & Lacroute, F. Interference of nonsense mutations with eukaryotic messenger RNA stability. *Proc. Natl. Acad. Sci. USA* **76**, 5134–5137 (1979).
4. Noensie, E.N. & Dietz, H.C. A strategy for disease gene identification through nonsense-mediated mRNA decay inhibition. *Nat. Biotechnol.* **19**, 434–439 (2001).
5. Huusko, P. *et al.* Nonsense-mediated decay microarray analysis identifies mutations of *EPHB2* in human prostate cancer. *Nat. Genet.* **36**, 979–983 (2004).
6. Dybbs, M., Ngai, J. & Kaplan, J.M. Using microarrays to facilitate positional cloning: identification of tomosyn as an inhibitor of neurosecretion. *PLoS Genet.* **1**, 6–16 (2005).
7. Meindl, A. *et al.* A gene (*RPGR*) with homology to the RCC1 guanine nucleotide exchange factor is mutated in X-linked retinitis pigmentosa (RP3). *Nat. Genet.* **13**, 35–42 (1996).
8. Schwahn, U. *et al.* Positional cloning of the gene for X-linked retinitis pigmentosa 2. *Nat. Genet.* **19**, 327–332 (1998).
9. Gu, J.J., Spychala, J. & Mitchell, B.S. Regulation of the human inosine monophosphate dehydrogenase type I gene. Utilization of alternative promoters. *J. Biol. Chem.* **272**, 4458–4466 (1997).
10. Vithana, E.N. *et al.* A human homolog of yeast pre-mRNA splicing gene, *PRP31*, underlies autosomal dominant retinitis pigmentosa on chromosome 19q13.4 (RP11). *Mol. Cell* **8**, 375–381 (2001).
11. McKie, A.B. *et al.* Mutations in the pre-mRNA splicing factor gene *PRPC8* in autosomal dominant retinitis pigmentosa (RP13). *Hum. Mol. Genet.* **10**, 1555–1562 (2001).
12. Chakarova, C.F. *et al.* Mutations in *HPRP3*, a third member of pre-mRNA splicing factor genes, implicated in autosomal dominant retinitis pigmentosa. *Hum. Mol. Genet.* **11**, 87–92 (2002).
13. Kim, Y.O. *et al.* Assignment of mitochondrial NAD+-specific isocitrate dehydrogenase beta subunit gene (*IDH3B*) to human chromosome band 20p13 by *in situ* hybridization and radiation hybrid mapping. *Cytogenet. Cell Genet.* **86**, 240–241 (1999).
14. Ramachandran, N. & Colman, R.F. Chemical characterization of distinct subunits of pig heart DPN-specific isocitrate dehydrogenase. *J. Biol. Chem.* **255**, 8859–8864 (1980).
15. Dolphin, D., Poulson, R. & Avramovic, O. *Pyridine Nucleotide Coenzymes* Part B, *Coenzymes and Cofactors* 606 (Wiley-Interscience, New York, 1987).
16. Cohen, P.F. & Colman, R.F. Diphosphopyridine nucleotide dependent isocitrate dehydrogenase from pig heart. Characterization of the active substrate and modes of regulation. *Biochemistry* **11**, 1501–1508 (1972).
17. Soundar, S., Park, J.H., Huh, T.L. & Colman, R.F. Evaluation by mutagenesis of the importance of 3 arginines in alpha, beta, and gamma subunits of human NAD-dependent isocitrate dehydrogenase. *J. Biol. Chem.* **278**, 52146–52153 (2003).
18. Garrett, R.H. & Grisham, C.M. *Biochemistry* 618 (Brooks Cole, Belmont, California, USA, 2004).
19. Hoek, J.B. & Rydstrom, J. Physiological roles of nicotinamide nucleotide transhydrogenase. *Biochem. J.* **254**, 1–10 (1988).
20. Moyle, J. & Mitchell, P. The proton-translocating nicotinamide-adenine dinucleotide (phosphate) transhydrogenase of rat liver mitochondria. *Biochem. J.* **132**, 571–585 (1973).
21. Smith, C.M. & Plaut, G.W. Activities of NAD-specific and NADP-specific isocitrate dehydrogenases in rat-liver mitochondria. Studies with D-threo-alpha-methylisocitrate. *Eur. J. Biochem.* **97**, 283–295 (1979).
22. Li, C. & Hung, W.W. Model-based analysis of oligonucleotide arrays: model validation, design issues and standard error application. *Genome Biol.* **2**, RESEARCH0032 (2001).
23. Warburg, O. & Christian, W. Isolierung und Kristallisation des Gärungsferments Enolase. *Biochem. Z.* **310**, 384–421 (1941).